

Synchronization Index of Neural Spike Trains in Response to Simulated Vowel Signal Stimuli in the Presence of a Pseudo-spontaneous Activity

Yoshimasa Wada, *Student Member IEEE*, and Hiroyuki Mino, *Senior Member IEEE*

Abstract—This article presents a statistical analysis of neural spike trains in an auditory nerve fiber (ANF) model stimulated extracellularly by simulated vowel electric stimuli under the case where a high-rate pulsatile waveform is presented as a conditioner for increasing the across-fiber-independency, i.e., desynchronization. In the computer simulation, stimulus current waveforms were presented repeatedly to a stimulating electrode located 1 mm above the 26th node of Ranvier, in an ANF axon model having 50 nodes of Ranvier, each consisting of stochastic sodium and potassium channels. From spike firing times recorded at the 36th node of Ranvier, the raster plots were depicted to explore the temporal precision and reliability of spike trains. Then the period histograms were generated to obtain the synchronization index defined using Shannon's entropy as a distance between the period histogram and the vowel electric stimuli. In the present article, it is shown that at a specific amplitude of simulated vowel waveforms, the possibility to encode the vowel signals with various amplitudes became greater, as well as the synchronization index was found to be maximized. It was implied that setting the amplitude of vowel signals to the specific values which maximize the synchronization index might contribute to efficiently encoding information on vowel formants under the high-rate pulsatile stimulation in cochlear prostheses.

Index Terms—Action Potential, Neural Spike Trains, Stochastic Ion Channels, Fluctuations, Electric Stimulation, Neural Encoding, Synchronization Index, Information-Theoretic Analysis, Neural Prosthesis, Computer Simulation.

I. INTRODUCTION

Electrical stimulation has played a key role in restoring function to individuals with neurological impairment. For the analysis of the influence of electric stimulus parameters on nerve fiber excitation, computational models have been constructed. For instance, in studies of cochlear prostheses, an ANF axon model with nodes of Ranvier containing stochastic sodium and potassium channels has been developed to realize neural spike (action potential) time fluctuations observed in feline single-fiber experiments [1]. Some basic properties of the axon model have been studied with regards to the spatio-temporal variation of spike initiations in response to not only a single-pulse stimulus [1], but also a double-pulse (masker-probe) stimulus [2].

It is still unclear, however, how electric stimulus parameters could affect the temporal precision and reliability of neural spike trains, and how much an electrically stimulated

ANF axon model could convey information about vowel formants under the case where a high-rate pulsatile waveform is presented as a conditioner for increasing the across-fiber-independency, i.e., desynchronization [4]. We note here that the high-rate pulsatile stimulation generates a pseudo-spontaneous activity of spike firings in deaf ear, instead of a spontaneous activity due to random secretions of synaptic vesicles in inner hair cells in healthy ear. The knowledge of the influence of electric stimulus parameters on the statistics of spike firing patterns might give us an insight to understanding how information about vowel formants can be encoded in an electrically stimulated ANF axon model [6].

This article presents a statistical analysis of spike firing patterns in a nerve fiber axon model from the viewpoint of electric stimulation for neural prostheses. The synchronization index of neural spike trains in response to simulated vowel signal with some amplitudes under the high-rate pulsatile stimulation for desynchronization is investigated by using the ANF axon model developed earlier in [1].

II. METHODS

ANFs were represented by a multi-compartment cable model with 50 nodal sections as described in [1]. The 50 nodes of Ranvier consisted of stochastic ion channels, 180 sodium channels, and 100 potassium channels, in order to generate plausible neural responses, like those observed in cat single-fiber experiments. The stochastic ion channels were implemented by the computationally efficient channel-number-tracking algorithm [3].

The transmembrane potentials of 200 ms in time length were generated for each simulation in which sampling steps were set at 2 μ s. As shown in Figure 1 (a), a stimulating electrode was located at a distance of 1 mm above the center node (26th), while a recording electrode was placed at the 36th node of Ranvier to measure the transmembrane potential, $V_m(36, t)$, as functions of space and time. Figure 1 (b) depicts the transmembrane potentials, of 100 ms in time length, recorded at the 36th node of Ranvier (top), the stimulus current waveform (middle), and the simulated vowel signal (bottom).

The stimulus current waveform, $I_{stim}(t)$, of 200 ms in time length was composed of a high-rate pulsatile conditioner with a rate of 5 kHz and a pulse duration of 40 μ s (0-200 ms), and the simulated vowel signal with a fundamental frequency of 100 Hz (20-200 ms). The vowel signal /a/ was synthesized using a cascade model [5] as follows: a pulse train with a fundamental frequency of 100 Hz was

Y. Wada is with Graduate School of Engineering, Kanto Gakuin University, 1-50-1 Mitsuura E., Kanazawa-ku, Yokohama 236-8501, Japan yoshiwada@zpost.plala.or.jp H. Mino is with Department of Electrical and Computer Engineering, Kanto Gakuin University, 1-50-1 Mitsuura E., Kanazawa-ku, Yokohama 236-8501, Japan mino@ieee.org

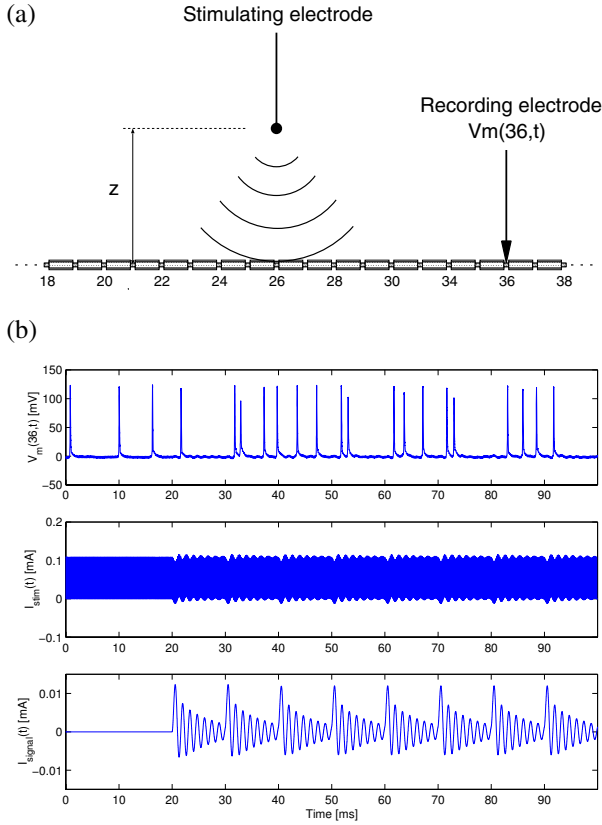


Fig. 1. (a) The configuration of electrodes and auditory nerve fiber model, where the node numbers are shown below the fiber. The stimulating electrode was located at the distance z of 1 mm above the center node (26th) of Ranvier, while the recording electrode was placed at the 36th node of Ranvier to measure the transmembrane potential as functions of space and time, $V_m(36, t)$'s. The stimulating current creates a variation in electric fields between the electrode and the fiber, as suggested by the arcs. (b) The top shows the transmembrane potentials, $V_m(36, t)$'s, in mV as a function of time (0-100 ms) in which $V_m(36, t)$'s are relative to the resting potential. The middle depicts the stimulus waveform, $I_{stim}(t)$, which consists of a pulsatile waveform with a rate of 5 [kHz] and a pulse duration of 40 [μ s] as well as a simulated vowel signal, $I_{signal}(t)$, with a fundamental frequency of 100 [Hz] and an amplitude factor of 20 (20-100 ms). The bottom shows $I_{signal}(t)$.

passed through a cascade of two single-pole glottal-pulse filters with a pole frequency of 250 Hz, and a two-pole formant filter with a formant frequency of 730 Hz and a bandwidth of 50 Hz. The vowel signal consisting of the first formant component was synthesized. Note that the stimulus current waveform of 0-20 ms was used as a pre-conditioning stimulus for generating a pseudo-spontaneous activity of spike firings. The amplitude of the pulsatile conditioner was set (109 μ A) such that the rate of pseudo-spontaneous spike firings was 110-120 Hz, while the amplitude scaling factor was varied (5, 10, 14, 17, 20, 30, and 40) to figure out how the encoding of the vowel signal into the ANF model can be influenced by the amplitude factors. One hundred samples of such stimuli were generated for calculating the statistical analysis (synchronization index defined below).

Each stimulus of one hundred stimuli was presented to the ANF model via the stimulating electrode, and in the meantime the transmembrane potentials were recorded at the 36th node of Ranvier.

Spike occurrence time was detected by determining when the transmembrane potential took the peak amplitude and was greater than 50% of the peak amplitude of typical action potentials. The spike times within 20-200 ms were used for statistical analysis.

The synchronization index (SI) % was calculated from the entropy of the period histogram (PH) and the entropy of the impulse response function of glottal and formant filters as follows:

$$SI = 100 \left(1 - \frac{|H_{vowel}(\theta) - H_{period}(\phi)|}{H_{vowel}(\theta)} \right) \quad (1)$$

where

$$H_{vowel}(\theta) = - \sum_{i=0}^{N-1} p(\theta_i) \log_2 p(\theta_i) \quad (2)$$

where θ_i denotes a function that the impulse response function of the glottal and formant filters is truncated to positive values, and where

$$H_{period}(\phi) = - \sum_{i=0}^{N-1} p(\phi_i) \log_2 p(\phi_i) \quad (3)$$

in which ϕ stands for the latency of spike firing times within one cycle of the fundamental frequency of the vowel signal.

III. RESULTS

Figure 2 shows the stimulus current waveform (top), the raster plot of thirty trials (middle), and the post-stimulus time histogram (bottom) are shown in each figure, (a)-(d). The amplitude factor of the simulated vowel signal with a fundamental frequency of 100 Hz was set at 10 in (a), 14 in (b), 20 in (c), and 30 in (d), respectively, in the presence of a pulsatile conditioner with a rate of 5 kHz and a pulse duration of 40 μ s. It is shown in the raster plots and PST histograms in 20-100 ms that the ANF model looks not to respond to the sinusoids in (a), tends to respond to various amplitude levels (a large value of dynamic range) in (b) and (c), and looks to respond too much to larger values of the amplitude of the vowel signal in (d).

Figure 3 shows the period histogram generated by collecting the spike firing times within one cycle of the simulated vowel signal of 100 Hz at the amplitude factors of 10 in (a), 14 in (b), 20 in (c), and 30 in (d) with a pulsatile conditioner having a rate of 5 kHz and a pulse duration of 40 μ s. The period histogram in (a) looks not to significantly appear a periodical component of spike firings, while those in (b)-(d) tend to respond to the simulated vowel signal. However, we note that the peak of the period histograms in (c) and (d) tends to be greater than the vowel function, suggesting that a larger amplitude factor would not necessarily play a role in better encoding information about the vowel formants.

Figure 4 summarizes the synchronization index % as a function of the amplitude factors at 5, 10, 14, 17, 20, 30, and 40. From the curve, it follows that the synchronization

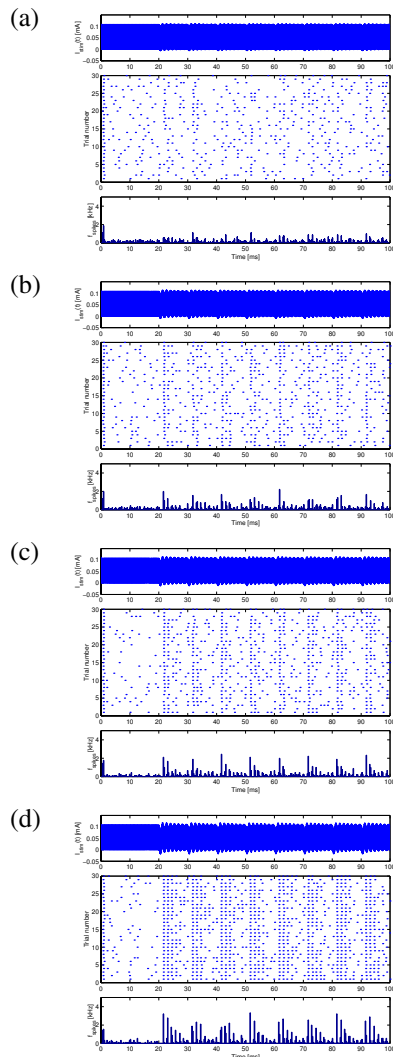


Fig. 2. The stimulus current waveform (top), the raster plot of thirty trials (middle), and the post-stimulus time histogram (bottom) are shown in each figure. The amplitude factor of the simulated vowel signal with a fundamental frequency of 100 Hz was set at 10 in (a), 14 in (b), 20 in (c), and 30 in (d), respectively, in the presence of a pulsatile conditioner with a rate of 5 kHz and a pulse duration of $40\ \mu s$. The PST histograms in 20-100 ms tend to be phase-locked as the amplitude factor of the simulated vowel signal increases in (a)-(d).

index was maximized at which the amplitude factor was set at 20.

IV. DISCUSSION AND CONCLUSION

In the present article, we have investigated the synchronization index of neural spike trains in an ANF axon model, with nodes of Ranvier consisting of stochastic sodium and potassium channels in which a simulated vowel signal was presented as stimuli to the ANF axon model in the presence of the pseudospontaneous activity of spike firings due to a high-rate pulsatile conditioner. We have shown that at a specific amplitude of the vowel signal, the possibility to encode the vowel signal with various amplitude levels

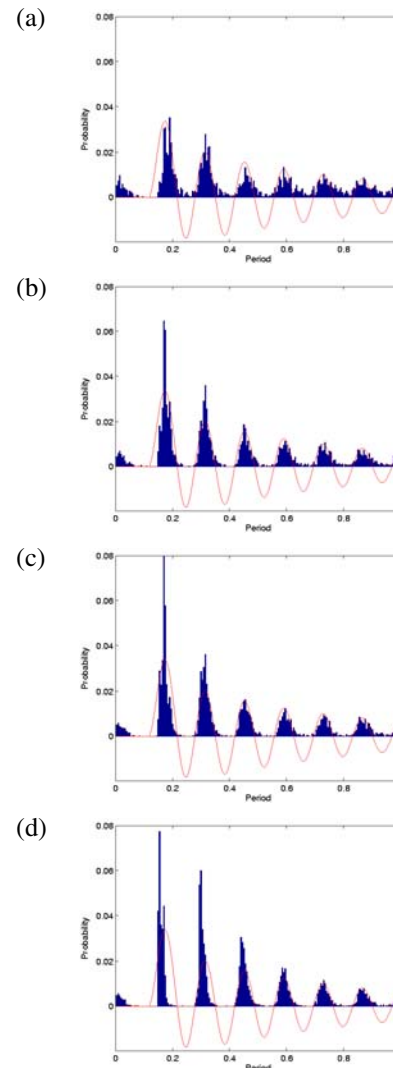


Fig. 3. The period histogram and the simulated vowel signal of one cycle at the amplitude factors of 10 in (a), 14 in (b), 20 in (c), and 30 in (d) with a pulsatile conditioner having a rate of 5 kHz and a pulse duration of $40\ \mu s$.

became greater as well as the synchronization index was found to be maximized.

It is implied that setting the amplitude parameter to some specific values makes it possible to efficiently encode information on vowel formants to the neural spike trains in the ANF axon model. Therefore, these modeling endeavors may significantly advance our understanding of information transfer in an electrically stimulated ANF axon model, and accelerate the design of better stimulus current waveforms on the basis of information-theoretic criteria for neural prostheses.

REFERENCES

[1] H. Mino, J.T. Rubinstein, C.A. Miller, and P.J. Abbas, "Effects of Electrode-to-Fiber Distance on Temporal Neural Response with Electrical Stimulation," *IEEE Trans. on Biomed. Eng.*, 51, pp.13-20, 2004.

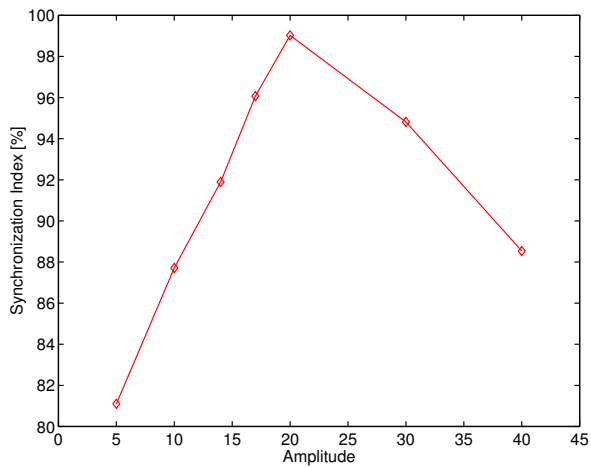


Fig. 4. Synchronization index % as a function of the amplitude factors at 5, 10, 14, 17, 20, 30, and 40.

- [2] H. Mino and J.T. Rubinstein, "Influences of Neural Refractoriness on Spatio-Temporal spike Initiations with Pulsatile Electrical Stimulation," *Proceeding of 25th Annual International Conference of IEEE Engineering in Medicine and Biology Society*, Paper ID 133, CD-ROM version, 2003 (Cancun, Mexico).
- [3] H. Mino, J. T. Rubinstein, and J. A. White, "Comparison of Computational Algorithms for the Simulation of Action Potentials with Stochastic Sodium Channels," *Annals of Biomedical Engineering*, 30, pp.578-587, 2002.
- [4] J.T. Rubinstein, B.S. Wilson, C.C. Finley, C.C. and P.J. Abbas, "Pseudospontaneous activity: stochastic independence of auditory nerve fibers with electrical stimulation," *Hear. Res.*, 127, pp.108-118, 1999.
- [5] L. R. Rabiner, "Digital Formant Synthesizer for Speech-Synthesis Studies," *J. Acoust. Soc. Am.*, 43, pp.822-828, 1968.
- [6] L.M. Litvak, B. Delgutte, and D. K. Eddington, "Improved neural representation of vowels in electric stimulation using desynchronizing pulse trains," *J. Acoust. Soc. Am.*, 114, pp.2099-2111, 2003.